



# Reversed-phase thin-layer chromatography and ultra-performance liquid chromatography/mass spectrometry to estimate the drug likeness of phosphodiesterase 10A inhibitors with phthalimide core

Anna Czopek<sup>1</sup> · Paweł Żmudzki<sup>1</sup> · Monika Dąbrowska<sup>2</sup> · Małgorzata Starek<sup>2</sup> · Kamil Łątka<sup>3</sup> · Marek Bajda<sup>3</sup> · Anna Jaromin<sup>4</sup> · Monika Fryc<sup>1</sup> · Agnieszka Zagórska<sup>1</sup>

Received: 23 February 2024 / Accepted: 12 April 2024  
© The Author(s) 2024, corrected publication 2024

## Abstract

Lipophilicity is a physicochemical parameter well known as a decisive factor for predicting the successful development of a drug. Thus, a balance between potency and physicochemical properties during medicinal chemistry optimization is needed. In this study, the lipophilicity of isoindole-1,3(2*H*)-dione derivatives designed as phosphodiesterase 10A (PDE10A) inhibitors was determined by chromatographic [reversed-phase thin-layer chromatography (RP-TLC) and ultra-performance liquid chromatography/mass spectrometry (UPLC/MS)] and *in silico* methods. To assess the correlation between the obtained lipophilicity parameters, principal component analysis (PCA) was performed.  $\log P$  values obtained by chromatographic ( $\log P_{\text{RP-TLC}}$  and  $\log P_{\text{UPLC/MS}}$ ) and *in silico* methods were compared using the PCA method. The results of PCA revealed that  $\log P_{\text{UPLC/MS}}$  and *in silico* clogP provided by the ChemDraw program were highly correlated. Compounds' drug likeness was screened, and the pharmacokinetic properties were predicted. All the investigated compounds displayed drug-likeness properties, and they met the criteria of Lipinski's rule of five, which predicted the oral bioavailability of drug candidates. Analysis of the influence of physicochemical properties on the biological activity showed that the compounds with increased potency on PDE10A had significantly higher topological polar surface area (TPSA) values. The blood–brain barrier permeability and the hemolytic activity of model compound **18** were examined. The model compound **18** displayed no toxicity effect on erythrocytes in the hemolytic assay and good parallel artificial membrane permeability. The results showed that phthalimide compounds with benzimidazole moiety are a source of compound-targeted inhibition of PDE10A with balanced physicochemical and drug-likeness properties.

**Keywords** PDE10A inhibitors · Lipophilicity · Drug-likeness · Hemolytic activity · Principal component analysis · Blood–brain barrier permeability

✉ Anna Czopek  
anna.czopek@uj.edu.pl

<sup>1</sup> Department of Medicinal Chemistry, Faculty of Pharmacy, Jagiellonian University Medical College, Medyczna 9, 30-688 Kraków, Poland

<sup>2</sup> Department of Inorganic and Analytical Chemistry, Faculty of Pharmacy, Jagiellonian University Medical College, Medyczna 9, 30-688 Kraków, Poland

<sup>3</sup> Department of Physicochemical Drug Analysis, Faculty of Pharmacy, Jagiellonian University Medical College, Medyczna 9, 30-688 Kraków, Poland

<sup>4</sup> Department of Lipids and Liposomes, Faculty of Biotechnology, University of Wrocław, Joliot-Curie 14a, 50-383 Wrocław, Poland

## 1 Introduction

Developing a new drug from the idea to market approval takes years and costs over one billion dollars. However, the flip side of the drug discovery process is the unintentional level of failures of drug candidates in clinical trials. As a result, the pharmaceutical industry is focusing on lead compounds' physicochemical properties in the early stages of drug discovery and developing a way to mitigate more expensive clinical failures later [1]. One of the essential physicochemical parameters is lipophilicity, well known as a decisive factor for predicting the successful development of a drug. Lipophilicity is a crucial factor influencing passive transport through biological membranes and significantly impacts protein binding, drug–receptor interactions,

drug-related toxicity, and adverse effects. High lipophilicity and accompanying poor aqueous solubility cause new drug molecules to be unable to solubilize completely in aqueous media or have very low permeability. Thus, a balance between potency and physicochemical properties during medicinal chemistry optimization is needed [2]. Control of lipophilicity during compound optimization can be accomplished using lipophilic efficiency indices such as ligand lipophilicity efficiency (LLE), which links potency, and lipophilicity to estimate drug likeness [3].

Lipophilicity of a compound is measured by its distribution in a biphasic system liquid–liquid (partition coefficient in *n*-octanol and water, logP) or solid–liquid [retention on reversed-phase thin-layer chromatography (RP-TLC), reversed-phase high-performance liquid chromatography (RP-HPLC), or ultra-performance liquid chromatography coupled with mass spectrometry (UPLC/MS)]. The chromatographic methods were developed to overcome the limitations and difficulties of the direct method for measuring logP, and both produce a high number of chromatographic lipophilicity indices [4–9]. Besides the experimental techniques, computational approaches for predicting logP (in silico) values are extensively used. The final logP value of the unknown compound is obtained by summing over all fragment contributions depending on the algorithm used to establish the contribution of each fragment on logP. Examples of fragmentation/group contribution-based methods are clogP, AClogP, ALOGP, miLogP, KOWWIN, XLOGP2, and XLOGP3. However, comparing computed values with those provided by the experimental methods is important [10–12].

Lastly, we designed, synthesized, and biologically evaluated the library of isoindole-1,3(2*H*)-dione derivatives connected by one to five methylene linkers with various amines. Modifications of amine moiety consisted in changing the size of the heterocyclic ring, *e.g.*, from monocyclic (1*H*-imidazole and pyridine) to bicyclic amines (benzimidazole, 6,7-dimethoxy-1,2,3,4-tetrahydroisoquinoline, 1,2,3,4-tetrahydroisoquinoline, and decahydroisoquinoline). Moreover, a phenyl ring was chosen instead of a heterocyclic amine moiety to examine the effect of amine fragments on in vitro activity (Fig. 1) [13].

The described group of compounds (3–23) has been designed as potential inhibitors of phosphodiesterase 10A

(PDE10A) and serotonin receptor ligands. However, the results of radioligand binding affinity for 5-HT<sub>1A</sub> and 5-HT<sub>7</sub> receptors revealed that the tested compounds exhibited lack of receptor activity. In return, new compounds were classified as inhibitors of PDE10A. Among the investigated series, the highest inhibitory activity for PDE10A expressed as the half-maximal inhibitory concentration (IC<sub>50</sub>) values displayed benzimidazole derivatives (15, 17–19, 22). The chosen compounds showed good IC<sub>50</sub> values as follows: 15, 6.71 μM; 17, 1.00 μM; 18, 0.89 μM; 19, 4.31 μM; 22, 5.65 μM; in comparison with papaverine (5.76 μM) [13].

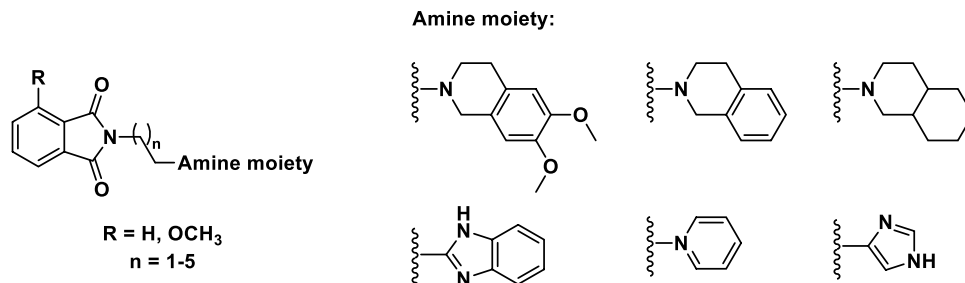
Knowing that lipophilicity is critical in optimizing hit molecules, the presented study aimed to determine the lipophilicity of 4-methoxy-1*H*-isoindole-1,3(2*H*)-dione derivatives. We decided to use RP-TLC and UPLC/MS retention data and in silico methods. The experimental results were compared with in silico calculated logP values parameters using the principal component analysis (PCA) method to assess the usefulness of computer programs for new compounds lipophilicity prediction. Next, based on the experimental results, all studied compounds' drug likeness was screened, and the pharmacokinetic properties were predicted. Finally, the blood–brain barrier permeability and the hemolytic activity of model compound 18 were analyzed.

## 2 Experimental

### 2.1 Investigated compounds, reference drugs, and materials

The small library of 4-methoxy-1*H*-isoindole-1,3(2*H*)-dione derivatives compounds (Fig. 1) was previously synthesized and in vitro characterized [13]. Reference drugs (purity > 99.5%) have been purchased from: Polfa Tarchomin (Warsaw, Poland) (barbital, phenobarbital), Alfa Aesar (Haverhill, MA, USA) (caffeine, benzocaine, phenytoin, and benzocaine), Sigma-Aldrich (St. Louis, MO, USA) (theobromine, theophylline, prednisolone, lidocaine, paracetamol, haloperidol, papaverine, acebutolol, furosemide, baclofen, ibuprofen, acetazolamide, amitriptyline, lorazepam, mefenamic acid, metronidazole, naphazoline, fluoxetine, promazine, propranolol, sulfasalazine, chlorpromazine,

**Fig. 1** The structures of the investigated compounds (3–23)



cinnarizine, and propranolol). Trazodone was extracted from Trittico CR tablets (Angelini Pharma, Rome, Italy). Liquid chromatography–mass spectrometry (LC–MS)-grade methanol and acetonitrile, 99.99% ammonium acetate, formic acid (> 98%), dimethyl sulfoxide (DMSO) were purchased from Sigma-Aldrich. LC–MS-grade 25% ammonium hydroxide solution was purchased from Fluka (Buchs, Switzerland).

## 2.2 RP-TLC chromatographic procedure

The mobile phases were prepared by mixing the respective amounts of water and methanol from 40% to 80% (V/V) in 5% increments. Methanol was used to prepare the solutions of the substances. RP-TLC was carried out on silica gel 60 RP-18 F<sub>254</sub> plates (Merck, Darmstadt, Germany). Solutions (10 µL) of the analyzed compounds were applied to the plates as 5 mm bands, 10 mm apart and 10 mm from the lower edge and sides of the plates, by using a Linomat 5 applicator (CAMAG, Muttenz, Switzerland). The vertical chamber (Sigma-Aldrich), 20 × 10 × 18 cm in size, was saturated with mobile phase for 20 min. Development was carried out over 9 cm from the starting line at a temperature of 20 °C. Next, the plates were dried at room temperature, and the spots were observed in ultraviolet light at 254 and/or 366 nm [ultraviolet (UV) lamp, CAMAG]. In each case, sharp and symmetric spots without a tendency for tailing were obtained. Each experiment was run in triplicate, and mean  $R_F$  (retardation factor) values were calculated. The  $R_M$  parameters were calculated using the equation  $R_M = \log(1/R_F - 1)$  starting from the  $R_F$  values. Linear correlations between the  $R_M$  values of the substances and the concentration of organic modifier in mobile phases were calculated using the equation  $R_M = R_{M0} + aC$ , where  $C$  is the concentration of the organic solvent (in %) in the mobile phase,  $a$  is the slope, and  $R_{M0}$  is the concentration of organic modifier extrapolated to zero.

## 2.3 UPLC/MS chromatographic procedure

The UPLC/MS system consisted of a Waters Acquity UPLC (Waters Corporation, Milford, MA, USA) coupled to a Waters TQD mass spectrometer (electrospray ionization mode ESI–tandem quadrupole). Chromatographic separations were carried out using the Acquity UPLC BEH (bridged ethyl hybrid) C<sub>18</sub> column; 2.1 × 100 mm, and 1.7 µm particle size, equipped with Acquity UPLC BEH C18 VanGuard pre-column; 2.1 × 5 mm, and 1.7 µm particle size. The column was maintained at 40 °C and eluted under isocratic conditions using from 10% to 70% in 5% intervals of eluent A over 30 min, at a flow rate of 0.3 mL min<sup>-1</sup>. Eluent A: water/buffer (10 mM ammonium acetate and ammonia to pH 7.4); eluent B: methanol. Methanol (UPLC grade), ammonium acetate (99.99%) and ammonia (UPLC grade)

were purchased from Sigma-Aldrich or Fluka. UPLC-grade water was obtained from an HLP 5 (Hydrolab, Warsaw, Poland) apparatus and was filtered through a 0.2 µm filter before use. Chromatograms were recorded using Waters eλ PDA detector. Spectra were analyzed in the 200–700 nm range with 1.2 nm resolution and a sampling rate of 20 points/s. One microliter of each of the solutions of the compounds or reference was injected. The data acquisition software was MassLynx V 4.1 (Waters Corporation). One milligram of each compound/reference was weighed and dissolved in 1 mL of a water–methanol mixture (1:1, V/V), making 1 mg mL<sup>-1</sup> stock solution. Samples were prepared by mixing 20 µL of the stock solutions and diluting the mixture to 1 mL, making a solution containing the investigated compounds in the concentration of 20 µL mL<sup>-1</sup>. Compounds were grouped to avoid preparing a mixture containing several compounds possessing similar  $m/z$  and that is isotopic.

## 2.4 In silico lipophilicity prediction

Theoretical octanol/water partition coefficients were calculated by use of the ChemDraw (ChemDraw 16.0, PerkinElmer Informatics Desktop Software, Waltham, MA, USA), SwissAdme online tool (<http://www.swissadme.ch/>), MarvinSketch (Marvin 20.10, ChemAxon, Budapest, Hungary) and Marvin (Marvin 17.6, ChemAxon).

## 2.5 Principal component analysis and statistical analysis

PCA and statistical parameters, such as correlation coefficient ( $R$ ), level of significance ( $p$ ), standard error of estimation ( $s$ ), and value of  $F$ -test of significance ( $F$ ), were determined in Statistica 13 (TIBCO Software Inc. 2017, Palo Alto, CA, USA). PCA was performed on experimental logP data sets, whereby the scores corresponding to the first principal component (PC1) were correlated with the values of computational (in silico) logP lipophilicity.

## 2.6 In silico drug likeness and pharmacokinetic properties prediction

The physicochemical properties of the studied compounds were calculated using QikProp (Small-Molecule Drug Discovery Suite 2017-3, Schrödinger, LLC, New York, NY, USA) programs and the SwissADME [14] website. Ligand lipophilicity efficiency (LLE) was calculated using the formula  $LLE = pIC_{50} - \log P$ , and binding efficiency index (BEI) was calculated using the equation  $BEI = pIC_{50}/MW$ , where  $pIC_{50}$  is the negative log of the half maximal inhibitory concentration ( $IC_{50}$ ) value expressed in moles,  $\log P$  is calculated the negative log of the partition coefficient ( $P$ ) value, and  $MW$  is a molecular weight expressed in kDa

[15]. Pharmacokinetic properties for the investigated compounds were predicted using the online pkCMS platform, which relies on distance/pharmacophore patterns encoded as graph-based signatures [16].

## 2.7 Parallel artificial membrane permeability assays

According to the manufacturer's procedure, the PAMPA assay was performed using Corning Gentest Pre-Coated PAMPA Plate System (Sigma-Aldrich) and UPLC–UV detection. Briefly, 50  $\mu\text{M}$  solutions of the analyzed compounds and reference compounds in PBS were prepared by diluting 1 mM stock solutions in DMSO with PBS. The 300  $\mu\text{L}$  of the resulting solutions were transferred to the wells of the donor plate, and the plate was placed on the acceptor plate containing 200  $\mu\text{L}$  of PBS per well. The assembly was incubated at 25  $^{\circ}\text{C}$  for 5 h, and afterwards, the concentrations of the compounds were assessed using the UPLC–UV method. The permeability was calculated using the equation

$$P_e = -\ln\left(1 - \frac{C_A(t)}{C_{\text{equilibrium}}}\right) : A \times \left(\frac{1}{V_D} + \frac{1}{V_A}\right) \times t,$$

where  $C_A$  = compound concentration in acceptor well at time  $t$ ,  $C_{\text{equilibrium}} = (C_D(t) \times V_D + C_A(t) \times V_A) / (V_D + V_A)$ ,  $C_D$  is the compound concentration in the donor well at time  $t$ ,  $V_A$  is the volume of the acceptor well (0.2 mL),  $V_D$  is the volume of the donor well (0.3 mL),  $A$  is the filter area (0.3  $\text{cm}^2$ ), and  $t$  is the incubation time (18,000 s). Each compound was analyzed in triplicate, and mean permeability was calculated.

## 2.8 Hemolytic activity

The hemolytic activity of **18** was evaluated by determining hemoglobin release from fresh human erythrocytes

according to the procedure described previously [17]. Compound **18** dissolved in DMSO was added in a volume corresponding to a final concentration of  $10^{-6}$ ,  $10^{-5}$ , or  $10^{-4}$  M and incubated with erythrocytes in PBS buffer at 37  $^{\circ}\text{C}$  for 30 min. After centrifugation, the released hemoglobin was determined spectrophotometrically at  $\lambda = 540$  nm. Negative (erythrocytes in PBS buffer), positive (erythrocytes in distilled water), and DMSO controls were also determined. The Bioethics Commission approved the study protocol at the Lower Silesian Medical Chamber (1/PNHAB/2018).

## 3 Results and discussion

### 3.1 Determination of lipophilicity

Experimental lipophilicity of the phthalimide derivatives **3–23** was determined by RP-TLC and UPLC/MS. The retention factors  $R_M$  (Tables 1AS, 1BS, 2AS, and 2BS in Supplementary Material) of the investigated compounds **3–23** obtained from RP-TLC decreased linearly with increasing methanol concentration in the mobile phase [from 40% to 80% (V/V) in 5% increments]. The experimental relative lipophilicity ( $R_{M0}$ ) and  $\log k_{\text{UPLC/MS}}$  values are presented in Table 1.

Based on the  $R_{M0}$ ,  $\log k$  values and literature data for reference compounds (Table 3S in Supplementary Material), we obtained equations (Fig. 2) and calculated  $\log P_{\text{RP-TLC}}$  and  $\log P_{\text{UPLC/MS}}$ , respectively. Based on these data, the  $\log P$  values of investigated compounds obtained using the RP-TLC method were in the range from 2.54 (compound **10**) to 6.35 (compound **7**), while obtained by UPLC/MS method ranged from 1.11 (compound **14**) to 5.62 (compound **5**) (Table 2).

In the case of  $\log P$  experimentally determined by the UPLC/MS method, the influence of substituents and the length of the carbon linker on lipophilicity is not so evident (Table 2). The lowest  $\log P$  values have compounds

**Table 1** The relative lipophilicity ( $R_{M0}$ ) values for tested compounds **3–23**

Compound	$R_{M0\text{RP-TLC}}^a$	$\log k_{\text{UPLC/MS}}^a$	Compound	$R_{M0\text{RP-TLC}}^a$	$\log k_{\text{UPLC/MS}}^a$
<b>3</b>	2.914	2.606	<b>14</b>	3.630	1.086
<b>4</b>	4.788	3.264	<b>15</b>	2.883	1.702
<b>5</b>	3.686	3.967	<b>16</b>	3.946	3.507
<b>6</b>	3.380	2.364	<b>17</b>	3.520	1.783
<b>7</b>	4.908	3.156	<b>18</b>	3.182	2.156
<b>8</b>	3.358	2.651	<b>19</b>	3.952	2.376
<b>9</b>	2.377	2.741	<b>20</b>	2.775	1.728
<b>10</b>	2.348	1.389	<b>21</b>	2.892	1.906
<b>11</b>	2.744	1.615	<b>22</b>	4.007	2.219
<b>12</b>	4.030	2.990	<b>23</b>	3.919	2.450
<b>13</b>	2.497	1.532			

<sup>a</sup> $r^2$  values were in the range of 0.81–0.99

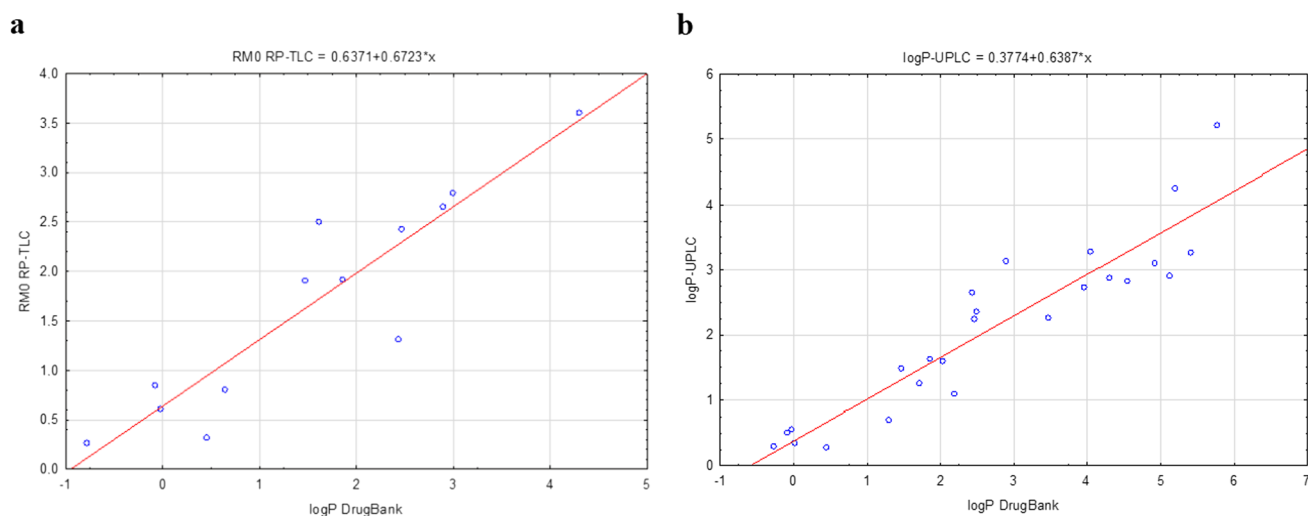


**Fig. 2** The relationship between logP from literature and experimental  $R_{M0}$  RP-TLC (**a** chart on the left;  $R=0.9163$ ,  $p<0.00001$ ,  $s=0.4495$ ,  $F=57.61$ ) and  $R_{M0}$  UPLC/MS (**b** chart on the right;  $R=0.9260$ ,  $p<0.000001$ ,  $s=0.5034$ ,  $F=138.35$ )

**Table 2** The experimental and computational partition coefficient for the investigated compounds **3–23**

Structure	Compound	<i>R</i>	<i>n</i>	logP	logP	clogP	logP	logP	logP <sub>SwissAdme</sub>	logP <sub>SwissAdme</sub>	
				RP-TLC	UPLC/MS	ChemDraw	Marvin (Consensus)	MarvinSketch	(XLOGP3)	Consensus	
	<b>3</b>	A	2	3.39	3.49	3.41	2.23	1.61	2.38	2.55	
	<b>4</b>	B	2	6.17	4.52	3.57	2.54	2.11	2.44	2.55	
	<b>5</b>	C	2	4.54	5.62	4.34	2.71	2.10	3.31	2.92	
	<b>6</b>	A	3	4.08	3.11	3.79	2.29	1.66	2.29	2.86	
	<b>7</b>	B	3	6.35	4.35	3.93	2.60	2.16	2.79	2.86	
	<b>8</b>	C	3	4.05	3.56	4.71	2.77	2.15	3.67	3.22	
	<b>9</b>	D	1	2.59	3.70	3.50	2.48	2.15	2.36	2.45	
	<b>10</b>	E	1	2.54	1.58	2.00	1.35	0.99	1.33	1.72	
	<b>11</b>	F	1	3.13	1.94	2.92	1.84	2.38	1.97	2.13	
	<b>12</b>	D	2	5.05	4.09	3.83	2.77	2.40	2.61	2.71	
	<b>13</b>	E	2	2.77	1.81	2.33	1.58	1.17	1.79	2.02	
	<b>14</b>	G	2	4.45	1.11	1.43	0.35	0.19	1.00	1.31	
	<b>15</b>	F	2	3.34	2.07	3.02	2.08	2.56	2.43	2.4	
	<b>16</b>	D	3	4.92	4.90	4.21	3.22	2.80	2.96	3.02	
	<b>17</b>	F	3	4.29	2.20	3.40	2.37	2.81	2.78	2.72	
	<b>18</b>	F	4	3.79	2.78	3.93	2.81	3.21	3.14	3.05	
	<b>19</b>	F	5	4.93	3.13	4.46	3.26	3.60	3.50	3.37	
		<b>20</b>	F	2	3.18	2.11	2.80	2.24	2.81	2.46	2.44
		<b>21</b>	F	3	3.35	2.39	3.18	2.53	3.06	2.81	2.75
<b>22</b>		F	4	5.01	2.88	3.71	2.97	3.46	3.17	3.08	
<b>23</b>		F	5	4.88	3.25	4.24	3.42	3.86	3.53	3.41	

A: 6,7-dimethoxy-3,4-dihydroisoquinolin-2(1H)-yl, B: 3,4-dihydroisoquinolin-2(1H)-yl, C: octahydroisoquinolin-2(1H)-yl, D: phenyl, E: pyridin-2-yl, F: 1H-benzo[d]imidazol-2-yl, G: 1H-imidazol-4-yl

with the following imidazole < pyridine < benzimidazole substituent, consistent with in silico results. For the derivatives with benzimidazole, phenyl, and pyridine fragments, the increase of predicted logP and elongation of the carbon

linker was also confirmed. However, for derivatives with decahydroisoquinoline, 1,2,3,4-tetrahydroisoquinoline, and 6,7-dimethoxy-1,2,3,4-tetrahydroisoquinoline substituents (compounds **3–8**), the effect of these fragments on



lipophilicity varied depending on the length of the carbon linker. In these cases, compounds with a three-carbon linker had lower lipophilicity than compounds with a two-carbon linker. Similarly, in experimentally determined logP values by the RP-TLC method, the increase in lipophilicity along with the elongation of the carbon linker is unambiguous in the case of decahydroisoquinoline and phenyl substituents (compounds **5** vs. **8** and **12** vs. **16**). However, for derivatives with 1,2,3,4-tetrahydroisoquinoline, 6,7-dimethoxy-1,2,3,4-tetrahydroisoquinoline, benzimidazole (except for compounds **17** and **22**) and pyridine fragments, the experimentally determined logP<sub>RP-TLC</sub> value increases with the elongation of the carbon linker. Moreover, compounds with a 4-methoxy group in phthalimide ring (**11**, **15**, **17–19**) showed slightly lower lipophilicity values, determined by RP-TLC and UPLC/MS methods, than their analogs without 4-methoxy substituent (**20–23**).

The in silico lipophilicity parameter was determined using the following programs: ChemDraw, Marvin, and MarvinSketch, as well as the Swiss ADME website module (Table 2) [18]. These programs use various calculation algorithms to increase the accuracy of logP prediction. Atomistic, topological, and hybrid methods (XLOGP3, MLOGP, Silicos-IT) are used, among others, to calculate in silico logP, and the mean value of the predicted methods used is called logP consensus.

Analysis of the clogP values for the investigated compounds (Table 2), it can be observed that regardless of the length of the carbon linker, the in silico predicted lipophilicity increases in the following order of moieties: imidazole < pyridine < benzimidazole < 1,2,3,4-tetrahydroisoquinoline < 6,7-dimethoxy-1,2,3,4-tetrahydroisoquinoline < phenyl/decahydroisoquinoline. Although logP values calculated using in silico methods generally correlate pretty well with those determined experimentally, one should draw detailed conclusions from them carefully. Possible incorrect predictions may result, among others, from the fact that the programs do not consider differences in the spatial conformation of compounds, which may significantly impact the observed lipophilicity within a specific group of compounds. The statistical analysis revealed that the clogP values obtained with the ChemDraw program showed the best correlation with logP determined by the UPLC/MS method ( $R = 0.7626$ ,  $p = 0.000058$ , Table 3).

It is important to note that logP RP-TLC values generally showed a slightly weaker correlation with logP calculated in silico compared with those obtained with UPLC/MS. The reason for the lower correlation between experimental and computational data in RP-TLC may be due to both the limitations of this technique (such as limited separation efficiency and limited sensitivity) and its inability to separate highly polar or ionized compounds. In

**Table 3** Correlation between calculated logP and logP values determined by the UPLC/MS method

Method	<i>R</i>	<i>p</i>	<i>s</i>	<i>F</i>
ChemDraw—CLogP	0.7626	0.000058	0.7806	26.41
Marvin—Consensus	0.6630	0.001053	0.9034	14.91
MarvinSketch—ChemAxon	0.2435	0.287488	1.1705	1.20
SwissAdme—XLOGP3	0.5791	0.005938	0.9838	9.59

*R* correlation coefficient, *p* level of significance, *s* standard error of estimation, *F* the value of the *F*-test of significance

**Table 4** Correlation between calculated logP and logP values determined by the RP-TLC method

Method	<i>R</i>	<i>p</i>	<i>s</i>	<i>F</i>
ChemDraw—CLogP	0.6380	0.002473	0.8758	12.36
Marvin—Consensus	0.6490	0.001960	0.8653	13.10
MarvinSketch—ChemAxon	0.3572	0.122041	1.0623	2.63
SwissAdme—XLOGP3	0.5322	0.015725	0.9629	7.11

*R* correlation coefficient, *p* level of significance, *s* standard error of estimation, *F* the value of the *F*-test of significance

the case of RP-TLC, the Marvin program provided the best results using the “consensus” option, rejecting one outlier point: compound **14** ( $R = 0.6490$ ,  $p = 0.001960$ , Table 4).

In the next step, multivariate statistics were performed using PCA to assess if there is any relationship between the experimental logP and computational logP variables. PCA is a chemometric technique that reduces the dimensionality of the original data set by finding the linear combinations of the variables called “principal components.” In the obtained new set, the variables were uncorrelated and ordered so that the first few components retain most of the variation in all original variables. As a result, the plot was obtained as a graphical representation of the PCA’s eigenvalues and proportions of explained variance. Based on the plot (Fig. 3a), it was decided to investigate the first two components (PC1 74.25% and PC2 14.95%), which explained approximately 89.2% of the data set’s variability.

The obtained results of PCA (Fig. 3b) revealed that calculated logP variables, provided by the Marvin program and the Swiss ADME website module, were highly correlated. Moreover, these data correlated reasonably well with logP obtained by MarvinSketch and ChemDraw programs. The predicted in silico logP did not correlate well with the experimental logP values. However, the analysis shows (Fig. 3b) that using the ChemDraw program to predict logP values in the tested group of compounds would be slightly better.

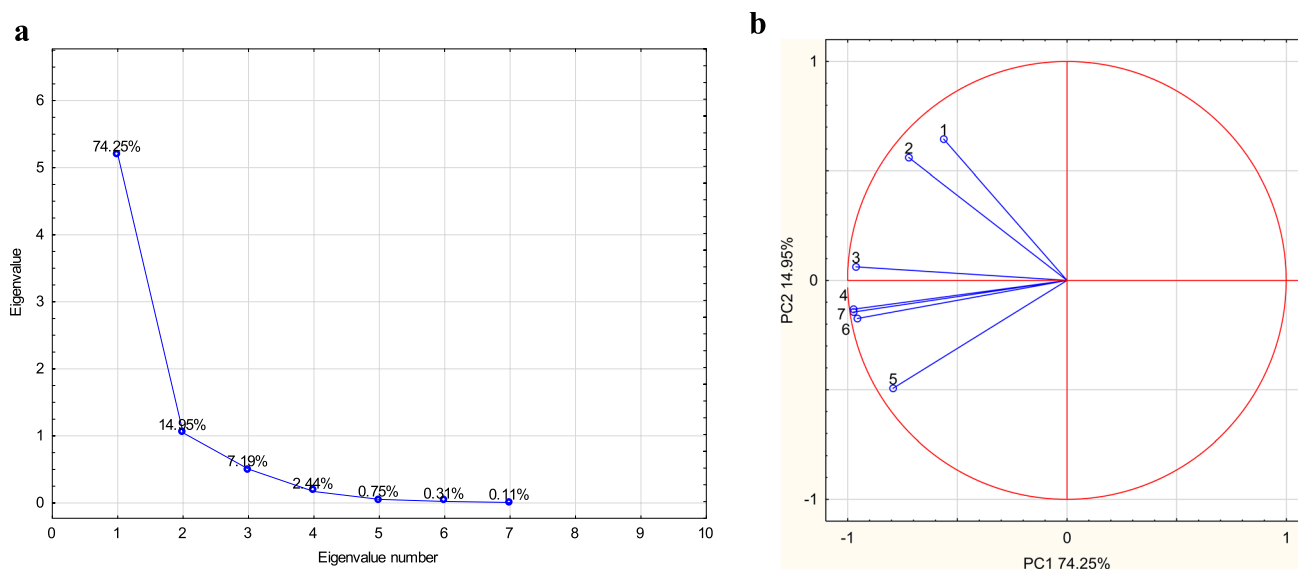


**Fig. 3** A screen plot of principal components in principal component analysis (a); PC1–PC2 score plots of logP<sub>RP-TLC</sub> and logP<sub>UPLC/MS</sub> and calculated partition coefficients (b): 1: logP<sub>RP-TLC</sub>; 2: logP<sub>UPLC/MS</sub>; 3: clogP<sub>ChemDraw</sub>; 4: logP<sub>Marvin (Consensus)</sub>; 5: logP<sub>MarvinSketch</sub>; 6: logP<sub>SwissAdme(XLOGP3)</sub>; 7: logP

### 3.2 Correlation of lipophilicity with PDE10A inhibition activity

In the case of the compounds with benzimidazole moiety, which displayed significant PDE10A inhibitory activity (15, 17–19), it could be observed that the PDE10A inhibition activity [13] increased with increasing lipophilicity determined by the UPLC/MS method, *i.e.*, with an elongation of the linker from one to four methylene groups. But then, despite the increase in lipophilicity associated with the further extension of the linker to five methylene groups, a decrease in inhibitory activity against PDE10A was observed. Moreover, despite slightly lower lipophilicity, compounds 11, 15, and 17–19 with 4-methoxy substituent in phthalimide ring showed higher activity than their analogs without 4-methoxy substituent (20–23).

### 3.3 Analysis of the influence of drug-likeness parameters on PDE10A activity

In the next step, the drug-likeness properties in line with the Lipinski “rule of five” (RO5) for the final compounds were assessed using the SwissAdme website (SI, Table 4S). The criteria of Lipinski rules are molecular weight (MW) ≤ 500 Da, lipophilicity values (logP) ≤ 5, number of hydrogen bond donors (NHD) ≤ 5, and number of hydrogen bond acceptors (NHA) ≤ 10 [19]. The logP values of the most tested compounds (either experimentally or computationally) meet the criteria for orally available drugs (logP < 5). Considering additionally the molecular weight

of the compounds (267.28–410.47, Table 4S, Supplementary Material) as well as the number of hydrogen bond donors (0–1) and hydrogen bond acceptors (3–6), all the studied compounds meet the criteria of Lipinski’s rule of five [19]. This suggests their good bioavailability after oral administration, which is also supported by the fact that they also fulfill Veber rules; thus, they have fewer than ten rotating bonds and a topological polar surface area (TPSA) value below 140 Å<sup>2</sup> [20, 21]. According to the BOILED-Egg diagram generated in SwissADME, most of the tested compounds (except compounds 11 and 14) can cross the blood–brain barrier due to their favorable TPSA (< 79 Å<sup>2</sup>) and logP (0.4–6.0) values [14]. This is also indicated by most compounds’ relatively low molecular weight (optimum ≤ 360) and the absence of only one hydrogen bond donor [22]. The studied compounds also fulfill the drug-likeness criteria proposed by Ghose, which, in addition to the logP mentioned above and molecular weight, also include molar refraction (optimum 40–130, studied compounds 74.65–119.57) and the total number of heavy atoms (optimum 20–70, studied compounds 20–30) [23].

Analysis of the influence of the physicochemical properties of the studied compounds on the activity toward particular biological targets showed that the compounds with increased potency on PDE10A had significantly higher TPSA values (Fig. 4). For the other properties, no meaningful correlations with activity were found.

Several lipophilicity indices have been introduced in recent years, which link a molecule’s lipophilicity or molecular weight with its activity and facilitate the

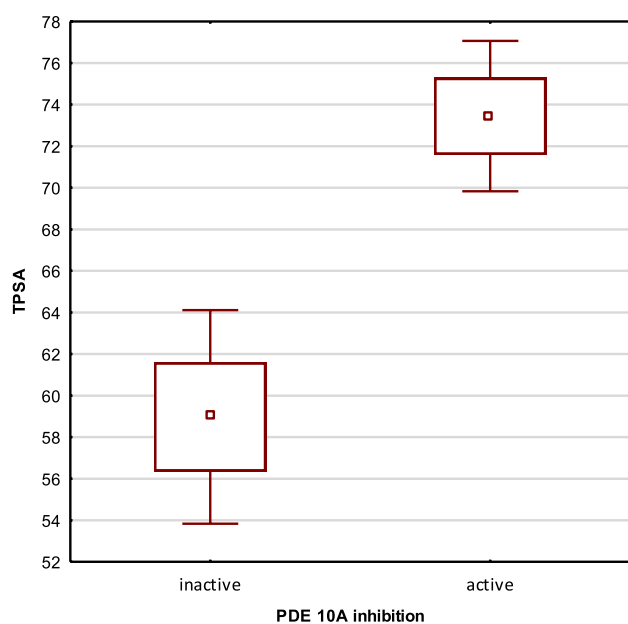


**Fig. 4** Comparison of TPSA values for active ( $\geq 40\%$  inhibition in  $10^{-5.5}$  M) and inactive compounds on PDE10A in Student's *t* test. TPSA mean value for inactive compounds 58.98, standard deviation (SD) 10.49; TPSA means value for active compounds 73.44, SD 4.13;  $p=0.00787$

selection of compounds for further research [15]. In this case, we calculated for the active compounds with benzimidazole moiety (**15**, **17–19**, **22**) two parameters: ligand lipophilicity efficiency (LLE) and binding efficiency index (BEI). The LLE parameter combines both potency and lipophilicity, whereas the BEI parameter relates to activity and molecular weight.

The LLE parameters of the tested compounds ranged from 0.24 to 2.26 for  $\log P_{\text{RP-TLC}}$  and from 2.24 to 3.80 for  $\log P_{\text{UPLC/MS}}$ , respectively (Table 5). The LLE values for the most active compound **18** were 2.26 and 3.27, respectively, deviating from the optimum of 5–7. The results were similar for the BEI parameter, where the optimum is between 20 and 30, and the tested compounds ranged from 14 to 18, with both compounds **17** and **18** showing the highest value of the BEI parameter ( $> 17$ ).

**Table 5** LLE and BEI parameters were calculated for the most active PDE10A inhibitors and reference drug—papaverine

Compound/drug	LLE <sub>RP-TLC</sub>	LLE <sub>UPLC/MS</sub>	BEI
<b>15</b>	1.83	3.10	16.10
<b>17</b>	1.71	3.80	17.89
<b>18</b>	2.26	3.27	17.32
<b>19</b>	0.44	2.24	14.77
<b>22</b>	0.24	2.37	16.43
Papaverine	2.04	–	15.44

### 3.4 Permeability assessment

Blood–brain barrier permeability studies are particularly crucial for compounds that exhibit activity in the central nervous system. In the early drug discovery process, optimization compounds are screened for their oral absorption to modify the physicochemical properties of hit compounds if they display poor permeability through membranes. Parallel artificial membrane permeability assays (PAMPA) have become helpful in predicting *in vivo* drug permeability [24]. In our case, it was used to predict the blood–brain barrier permeability of selected, the most potent compound **18**. Additionally, we tested nine commercially available drugs as phenobarbital, propranolol, theobromine, barbital, theophylline, mefenamic acid, naphazoline, loratadine, and sulfasalazine and classified their permeability through the blood–brain barrier as good to average (CNS+) or poor (CNS–), respectively (Table 6).

The PAMPA assay results are consistent with the *in silico* predictions for the blood–brain barrier permeability value of compound **18** described above. The results indicate that compound **18** can cross the blood–brain barrier and interact with PDE10A in the central nervous system.

### 3.5 Pharmacokinetic in silico prediction

In preliminary studies, the balance between activity and pharmacokinetic parameters is crucial for effective drug candidates [2]. Thus, computational approaches have been developed to optimize pharmacokinetic properties that allow the evaluation of these parameters for newly synthesized compounds. One of these predictive models was used to assess the *in silico* pharmacokinetic parameters of the investigated compounds **3–23** (for detailed information, please see Tables 5AS and 5BS in Supplementary Material) with a phthalimide core.

**Table 6** Permeability ( $\log P_c$ ) in the PAMPA assay and prediction of the CNS penetration

Drugs/compound	$\log P_c$	Prediction
Phenobarbital	–5.02	CNS+
Propranolol	–5.03	CNS+
Compound <b>18</b>	–5.29	CNS+
Theobromine	–5.44	CNS+
Barbital	–5.47	CNS+
Theophylline	–5.52	CNS+
Mefenamic acid	–4.61	CNS+
Naphazoline	$< -8$	CNS–
Loratadine	$< -8$	CNS–
Sulfasalazine	$< -8$	CNS–



The absorption of orally administrated drugs was assessed in the Caco-2 cell prediction model, in which all the compounds showed average predicted values ( $> 0.90$ ). The obtained prediction results revealed that the investigated compounds **3–23** would be absorbed from the intestinal truck ( $> 80\%$ ) but display relatively poor water solubility. The investigated compounds showed average predicted values in the blood–brain barrier permeability test ranging from  $-0.905$  to  $0.003$ , except for compound **14**, which is poorly distributed to the brain, probably due to good water solubility and low lipophilicity. According to prediction results, most compounds are P-glycoprotein substrates, whereas only a few compounds act as P-glycoprotein inhibitors. CYP3A4 likely metabolizes most investigated compounds but not CYP2D6. Moreover, tested compounds with monoamine cyclic moiety will probably be cytochrome CYP2D6 (**3–8**, **17–23**) inhibitors, whereas compounds with phenyl or pyridine and benzimidazole ring will be cytochrome CYP1A2 (**9**, **11–13**, **15–23**) or cytochrome CYP2C19 (**9**, **10**, **12**, **16–19**, **21–23**) inhibitors. In addition, compounds containing a benzimidazole moiety linked to a phthalimide fragment by a butyl or pentyl linker will probably inhibit CYP3A4 and CYP2C9 (**18**, **19**, **23**).

### 3.6 Hemolytic activity

An additional assay was taken to measure the potential toxicity toward mammalian cells, such as erythrocytes, for the most active compound **18**. Compounds with good permeability can damage the membrane, causing a structural destabilization of the membrane of red blood cells. Our test monitored the ability to lysis human erythrocytes by estimating the level of released hemoglobin. The results confirmed that **18** is safe for this type of cell, as no hemolysis was detected when used in the concentration range  $10^{-6}$ – $10^{-4}$  M. Our results follow findings obtained by Bogdanov et al. [25]. They found that isatin derivatives also do not have high hemolytic activity. Moreover, it also corresponds well with the results reported by Nayab et al., who proved that some N-substituted phthalimides showed less than 20% hemolysis [26]. Thus, the lack of toxicity **18** toward this type of human cell suggests that this compound is very promising for further studies.

## 4 Conclusions

This study determined the drug likeness of new compounds based on phthalimide core linked with various nitrogen-containing heterocycles (compounds **3–23**) using RP-TLC and UPLC/MS methods. Based on experimental and computational logP values, PCA confirmed the best correlation between logP determined by the UPLC/MS method

and in silico obtained logP using the ChemDraw program. Therefore, this program can be used for the most reliable prediction of lipophilicity in an analogous series of compounds. Interestingly, the compounds with benzimidazole moiety (**15**, **17–23**), which inhibit the PDE10A enzyme, had significantly higher TPSA values than the inactive compounds. Among them, the most potent compound **18** (2-[4-(1*H*-benzimidazol-2-yl)butyl]-4-methoxy-1*H*-isoin-dole-1,3(2*H*)-dione) was identified in permeability assessment using UPLC/MS PAMPA as a molecule that can cross the blood–brain barrier. Furthermore, compound **18** showed no hemolytic activity toward human erythrocytes in tested concentrations. In conclusion, the presented results showed that the drug likeness of complex compounds containing several bicyclic groups, including phthalimide, isoquinoline, or benzimidazole, is better characterized by the more precise and accurate UPLC/MS method.

**Supplementary Information** The online version contains supplementary material available at <https://doi.org/10.1007/s00764-024-00298-9>.

**Acknowledgements** This work was supported by the Statutory Activity of Jagiellonian University Medical College (N42/DBS/000020 and N42/DBS/000303).

**Funding** This work was supported by the Statutory Activity of Jagiellonian University Medical College (N42/DBS/000020 and N42/DBS/000303). The modernization of the UPLC/MS apparatus was funded by the Priority Research Area qLife under the program “Excellence Initiative—Research University” at the Jagiellonian University in Krakow.

## Declarations

**Competing interests** The authors declare that they do not have any conflict of interest and they have no competing interests to declare that are relevant to the content of this article.

**Ethical approval** The Bioethics Commission approved the study protocol at the Lower Silesian Medical Chamber (1/PNHAB/2018).

**Open Access** This article is licensed under a Creative Commons Attribution 4.0 International License, which permits use, sharing, adaptation, distribution and reproduction in any medium or format, as long as you give appropriate credit to the original author(s) and the source, provide a link to the Creative Commons licence, and indicate if changes were made. The images or other third party material in this article are included in the article's Creative Commons licence, unless indicated otherwise in a credit line to the material. If material is not included in the article's Creative Commons licence and your intended use is not permitted by statutory regulation or exceeds the permitted use, you will need to obtain permission directly from the copyright holder. To view a copy of this licence, visit <http://creativecommons.org/licenses/by/4.0/>.

## References

1. Lobo S (2019) Is there enough focus on lipophilicity in drug discovery? *Expert Opin Drug Discov* 15:261–263. <https://doi.org/10.1080/17460441.2020.1691995>

2. Miller RR, Madeira M, Wood HB et al (2020) Integrating the impact of lipophilicity on potency and pharmacokinetic parameters enables the use of diverse chemical space during small molecule drug optimization. *J Med Chem* 63:12156–12170. <https://doi.org/10.1021/acs.jmedchem.9b01813>
3. Leeson PD, Springthorpe B (2007) The influence of drug-like concepts on decision-making in medicinal chemistry. *Nat Rev Drug Discov* 6:881–890. <https://doi.org/10.1038/NRD2445>
4. Ciura K, Fedorowicz J, Andrić F et al (2019) Lipophilicity determination of antifungal isoxazolo[3,4-b]pyridin-3(1h)-ones and their n1-substituted derivatives with chromatographic and computational methods. *Molecules* 24:4311. <https://doi.org/10.3390/molecules24234311>
5. Zagórska A, Czopek A, Pełka K et al (2014) Reversed-phase TLC study of some long chain arylpiperazine of imidazolidine-2,4-dione and imidazo[2,1-f]purine-2,4-dione derivatives. *Acta Pol Pharm* 71:379–383
6. Chino A, Masuda N, Amano Y et al (2014) Novel benzimidazole derivatives as phosphodiesterase 10A (PDE10A) inhibitors with improved metabolic stability. *Bioorg Med Chem* 22:3515–3526. <https://doi.org/10.1016/j.bmc.2014.04.023>
7. Ayouni L, Cazorla G, Chaillou D et al (2005) Fast determination of lipophilicity by HPLC. *Chromatographia* 62:251–255. <https://doi.org/10.1365/s10337-005-0608-6>
8. Henchoz Y, Guillaume D, Rudaz S et al (2008) High-throughput log P determination by ultraperformance liquid chromatography: a convenient tool for medicinal chemists. *J Med Chem* 51:396–399. <https://doi.org/10.1021/jm7014809>
9. Žuvela P, Skoczylas M, Jay Liu J et al (2019) Column characterization and selection systems in reversed-phase high-performance liquid chromatography. *Chem Rev* 119:3674–3729
10. Meylan WM, Howard PH (1995) Atom/fragment contribution method for estimating octanol–water partition coefficients. *J Pharm Sci* 84:83–92. <https://doi.org/10.1002/jps.2600840120>
11. Wang R, Gao Y, Lai L (2000) Calculating partition coefficient by atom-additive method. *Perspect Drug Discov Des* 19:47–66. <https://doi.org/10.1023/A:1008763405023>
12. Cheng T, Zhao Y, Li X et al (2007) Computation of octanol-water partition coefficients by guiding an additive model with knowledge. *J Chem Inf Model* 47:2140–2148. <https://doi.org/10.1021/ci700257y>
13. Czopek A, Partyka A, Bucki A et al (2020) Impact of N-alkylamino substituents on serotonin receptor (5-HT<sub>2</sub>) affinity and phosphodiesterase 10A (PDE10A) inhibition of isoindole-1,3-dione derivatives. *Molecules* 25:3868. <https://doi.org/10.3390/molecules25173868>
14. Daina A, Zoete V (2016) A BOILED-egg to predict gastrointestinal absorption and brain penetration of small molecules. *ChemMedChem* 11:1117–1121. <https://doi.org/10.1002/cmdc.201600182>
15. Kenny PW (2019) The nature of ligand efficiency. *J Cheminform* 11:1–18. <https://doi.org/10.1186/S13321-019-0330-2/FIGURES/1>
16. Pires DEV, Blundell TL, Ascher DB (2015) pkCSM: predicting small-molecule pharmacokinetic and toxicity properties using graph-based signatures. *J Med Chem* 58:4066–4072. <https://doi.org/10.1021/acs.jmedchem.5b00104>
17. Jaromin A, Korycińska M, Piętko-Ottlik M et al (2012) Membrane perturbations induced by new analogs of neocryptolepine. *Biol Pharm Bull* 35:1432–1439. <https://doi.org/10.1248/bpb.b110671>
18. Daina A, Michielin O, Zoete V (2017) SwissADME: a free web tool to evaluate pharmacokinetics, drug-likeness and medicinal chemistry friendliness of small molecules. *Sci Rep* 7:1–13. <https://doi.org/10.1038/srep42717>
19. Lipinski CA, Lombardo F, Dominy BW, Feeney PJ (2001) Experimental and computational approaches to estimate solubility and permeability in drug discovery and development settings. *Adv Drug Deliv Rev* 46:3–26. [https://doi.org/10.1016/S0169-409X\(00\)00129-0](https://doi.org/10.1016/S0169-409X(00)00129-0)
20. Veber DF, Johnson SR, Cheng H-Y et al (2002) Molecular properties that influence the oral bioavailability of drug candidates. *J Med Chem* 45:2615–2623. <https://doi.org/10.1021/jm020017n>
21. Egan WJ, Merz KM, Baldwin JJ et al (2000) Prediction of drug absorption using multivariate statistics. *J Med Chem* 43:3867–3877. <https://doi.org/10.1021/jm000292e>
22. Wager TT, Hou X, Verhoest PR, Villalobos A (2010) Moving beyond rules: the development of a central nervous system multiparameter optimization (CNS MPO) approach to enable alignment of druglike properties. *ACS Chem Neurosci* 1:435–449. <https://doi.org/10.1021/cn100008c>
23. Ghose AK, Viswanadhan VN, Wendoloski JJ (1999) A knowledge-based approach in designing combinatorial or medicinal chemistry libraries for drug discovery. 1. A qualitative and quantitative characterization of known drug databases. *J Comb Chem* 1:55–68. <https://doi.org/10.1021/cc9800071>
24. Avdeef A (2012) Absorption and drug development: solubility, permeability, and charge state. Wiley, New York
25. Bogdanov AV, Voloshina AD, Sapunova AS et al (2020) Effect of structure of 1-substituted isatins on direction of their reactions with some acetohydrazide ammonium derivatives. *Russ J Gen Chem* 90:1591–1600. <https://doi.org/10.1134/S1070363220090029>
26. Nayab PS, Irfan M, Abid M et al (2017) Experimental and molecular docking investigation on DNA interaction of N-substituted phthalimides: antibacterial, antioxidant and hemolytic activities. *Luminescence* 32:298–308. <https://doi.org/10.1002/bio.3178>